JOURNAL OF Applied Polymer SCIENCE

Special Issue: Sustainable Polymers and Polymer Science Dedicated to the Life and Work of Richard P. Wool

Guest Editors: Dr Joseph F. Stanzione III (Rowan University, U.S.A.)
and Dr John J. La Scala (U.S. Army Research Laboratory, U.S.A.)

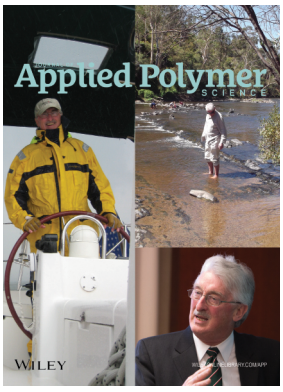

EDITORIAL

REVIEWS

RESEARCH ARTICLES

JOURNAL OF Applied Polymer SCIENCE

Special Issue: Sustainable Polymers and Polymer Science Dedicated to the Life and Work of Richard P. Wool

Guest Editors: Dr Joseph F. Stanzione III (Rowan University, U.S.A.)
and Dr John J. La Scala (U.S. Army Research Laboratory, U.S.A.)

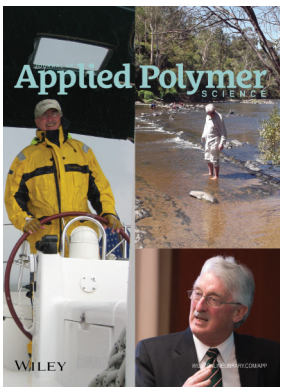

Journal of Applied Polymer Science

Evaluation of the emulsion copolymerization of vinyl pivalate and methacrylated methyl oleate

Alan Thyago Jensen,[1] Ana Carolina Couto de Oliveira,[1] Sílvia Belém Gonçalves,[2] Rossano Gambetta,[2] Fabricio Machado[1]

[1]Instituto de Química, Universidade de Brasília, *Campus* Universitário Darcy Ribeiro, CP 04478, Brasília, 70910-900 DF, Brazil
[2]Embrapa Agroenergia, Parque Estação Biológica, PqEB s/n, W3 Norte, CEP 70770-901, Brasília, DF, Brazil
Correspondence to: F. Machado (E-mail: fmachado@unb.br)

ABSTRACT: In this study, we synthesized a new class of copolymeric lattices based on vinyl pivalate (VPi) and modified oleic acid (OA) through a batch emulsion polymerization process. The effects of the chemically modified OA [methacrylated methyl oleate (MAMO)] on the thermal stability, glass-transition temperature (T_g), average molar masses [mass-average molar mass (M_w) and number-average molar mass (M_n)], and molar mass dispersity ($Đ$) of the copolymers were evaluated. The experimental results indicate that via the introduction of MAMO into the polymer chains resulted in significant reductions in T_g, M_w, M_n, and $Đ$; this demonstrated a decrease of T_g at approximately 40 °C when the MAMO molar fraction equaled 9% compared to the value observed for the pure poly(vinyl pivalate) (PVPi), which was equal to 80.5 °C. MAMO incorporation led to a significant decrease in the M_w value observed in the interval, with a differential from approximately 1.6×10^3 to 289.6 kg/mol, and $Đ$ values between 2.17 to 1.55, which was when the MAMO molar fraction present in the VPi-containing copolymers varied from zero (pure PVPi) to approximately 9 mol %. We also observed that the thermal stability of the copolymers decreased slightly when the MAMO concentration increased in the reaction medium. Despite this minor drawback, polymer lattices with a high colloidal stability were formed at a high rate of polymerization, and the elevated conversion was within the interval 90–100%. © 2016 Wiley Periodicals, Inc. J. Appl. Polym. Sci. **2016**, *133*, 44129.

KEYWORDS: addition polymerization; biopolymers and renewable polymers; copolymers; emulsion polymerization; properties and characterization

Received 6 February 2016; accepted 27 June 2016
DOI: 10.1002/app.44129

INTRODUCTION

Vinyl pivalate (VPi) homopolymerization has been widely evaluated with the intention of producing spherical poly(vinyl pivalate) (PVPi) or core–shell particles of PVPi/poly(vinyl alcohol) with a high syndiotacticity[1–8] through a heterogeneous suspension polymerization processes. Despite the use of suspension polymerization in the synthesis of microsized VPi-based polymers, the application of these polymeric materials are limited because of undesirable features, such as relatively low average molar masses, in the polymeric chains and the micrometric scale of the polymer particles.

The technical limitations mentioned previously were observed when PVPi was produced through both bulk and suspension polymerization; it could be minimized when heterogeneous emulsion polymerization processes were used to produce VPi-based polymeric materials. This represented significant improvements in the polymer quality, as high reaction rates and polymer chains with high molar masses could be easily achieved.[9,10] Song and Lyoo[11] synthesized PVPi, which exhibited a high average molar mass at temperatures in the range from 50 to 55 °C, with 2,2′-azobis(2-amidinopropane) dihydrochloride as the initiator of the polymerization reactions, which were carried out in an emulsion polymerization system and led to the formation of PVPi with an elevated chain linearity and high polymer yield.

Kikuchi *et al.*[12] studied the effect of the electrolytes sodium sulfate, potassium sulfate, lithium sulfate monohydrate, sodium chloride, ammonium acetate, sodium acetate, diammonium hydrogen citrate, tetramethylammonium chloride, and anhydrous lithium chloride and their influence on the reaction behavior of the emulsion polymerization of VPi. According to Kikuchi *et al.*,[12] the stability of the reaction system and the particle size distribution were strongly influenced by the type of ion and the ionic strength of the electrolytes. Kwark *et al.*[13] evaluated the vinyl acetate (VAc)/VPi copolymerization performed in a redox emulsion process, with manganese chelate as the initiator of the reaction. In this study, a copolymerization model was proposed, and it was shown to be able to predict the experimental data of the copolymerization fairly well.

It is well known that the polymerization of vinyl monomers through emulsion systems typically leads to polymers composed of very long chains. Suzuki *et al.*[14] evaluated the effect of the chain-transfer agents *n*-dibutyl disulfide, *t*-dibutyl disulfide, and L-cystein on both the kinetic behavior and particle nucleation during VPi emulsion polymerizations. According to the experimental results, the use of the chain-transfer agents led to a decrease in both the average molar masses and the average particle size of PVPi formed in the aqueous phase.

Taking into account that some polymers of very elevated molar mass might have represented strong limitations to the application of the final polymer because of the high amount energy consumed during its processing, the use of chemically modified vegetable oils in the synthesis of copolymeric materials with tailored molar masses and glass-transition temperature (T_g) values may be considered as a very interesting and viable strategy for the emulsion polymerization processes.[15,16]

With respect to these properties, the use of vegetable oils as new sources of monomeric precursors of polymeric materials has become more emergent because of the following reasons: its renewable source of origin, high availability, and low cost. Additionally, we want to highlight its high potential to undergo chemical modification of unsaturated fatty acids, such as oleic, linoleic, linolenic, and ricinoleic acids, which can be found at elevated concentrations in the composition of several vegetable oils.[15,17–20] Such raw materials may be very appealing to the polymer industry for use in the formulation of different materials, such as paints, adhesives, resins, nanocomposites, thermoplastics, and thermosets.[20–25]

The use of modified oleic acid (OA) in combination with glycidyl methacrylate with originating polymer latexes consisting of a high gel level, as described by Moreno *et al.*,[26] has demonstrated the high demand for the production of environmentally friendly polymeric materials for use in architectural coatings. Polymeric lattices synthesized through emulsion polymerization processes, described by Jensen *et al.*[16] and Ferreira *et al.*,[15] are examples of combinations of vinyl monomers and comonomers derived from vegetable oils. In these studies, the formation of styrene/acrylated methyl oleate copolymers and soybean-oil-based copolymers [containing a mixture of acrylated linolenic acid, linoleic acid, and OA in combination with methyl methacrylate (MMA)] were studied; the studies indicated that the derived vegetable oil comonomer significantly affected the thermal stability, T_g, average molar mass, and molar mass distribution (MMD) of the copolymers based in styrene[16] and MMA.[15]

The application of OA as a (co)monomeric species in free-radical polymerization systems requires a modification to its chemical structure. The functionalization of the chemical structure of the unsaturated precursor plays a significant role, as the modified species will contain a functional group that will easily undergo polyaddition in homogeneous and heterogeneous processes.[22,27–30] With respect to VPi, a quality improvement of VPi-containing polymers can be achieved when an emulsion polymerization process is used compared to when bulk and suspension polymerization processes are used.[11,13]

In this study, the emulsion copolymerization of VPi and methacrylated methyl oleate (MAMO) were conducted at different compositions to produce copolymeric lattices with designed average molar masses and T_g values in reactions exhibiting high polymer yields. The effects of the process variables, such as the concentrations of the polymerization initiator and emulsifier, on the reaction conversion, average molar masses, and particle size were investigated. We expected that the synthesis of poly(vinyl pivalate-*co*-methacrylated methyl oleate) [PVPiMAMO] would provide a new perspective with respect to the production of polymeric materials of high industrial interest, for example, inks and adhesives. To the best of our knowledge, no other previous publications in the open literature present experimental data for the VPi/MAMO emulsion copolymerization.

EXPERIMENTAL

Materials

OA ($C_{18}H_{32}O_2$) was supplied by Synth. Methyl alcohol (CH_3OH) was supplied by Vetec Química Fina, Ltd. (Rio de Janeiro, Brazil). Sulfuric acid (H_2SO_4) was supplied by Vetec Química Fina. Formic acid (CH_2O_2) was supplied by Vetec Química Fina. Hydrogen peroxide (H_2O_2; 30%) was supplied by Merck. Methacrylic acid (MA; $C_3H_4O_2$) was supplied by Vetec Química Fina. Hydroquinone [$C_6H_4(OH)_2$], provided by Vetec Química Fina, was used to inhibit the polymerization in the samples withdrawn during the reaction. Isopropyl alcohol (C_3H_7OH) was provided by Dynamic Analytical Reagents. Toluene ($C_6H_5CH_3$) was supplied by Vetec Química Fina. Diethyl ether (C_2H_6O) was provided by Ecibra Analytical Reagents. VPi ($C_7H_{12}O_2$), supplied by Aldrich (Sigma-Aldrich do Brasil Ltd., São Paulo, Brazil), with a purity of 99%, was used as the monomer. Sodium bicarbonate ($NaHCO_3$) was supplied by Vetec Química Fina. Anhydrous magnesium sulfate ($MgSO_4$) was supplied by Vetec Química Fina. Anhydrous sodium sulfate (Na_2SO_4) was supplied by Vetec Química Fina. Potassium persulfate (KPS; $K_2S_2O_8$), supplied by Vetec Química Fina and with a purity of 99%, was used as the initiator of polymerization. Sodium lauryl sulfate (SLS; $NaC_{12}H_{25}SO_4$), supplied by Reagen, was used as the emulsifier. All chemicals were used as received without further purification.

Synthesis of MAMO

MAMO was obtained according to the experimental procedure described by Jensen *et al.*[16] and the reader is referred to this reference for more detailed information. Initially, a mixture containing OA and methanol in a molar ratio of 1:4 and 1% (w/w) H_2SO_4 was charged in a round-bottom flask connected to a reflux condenser along with a Pt100 thermocouple probe. The esterification reaction was carried out with reflux under strong magnetic agitation (1000 rpm) in an oil bath at 80 °C for 3 h. The procedure was repeated three times until a conversion of 96% of methyl oleate was achieved. The conversion values were verified with measurements of the acid value in accordance with American Oil Chemists' Society Official Method Cd 3d-63.

After the esterification procedure, the epoxidation of the double bond of methyl oleate was performed. The epoxidation reaction was performed with a mass proportion equal to 10:8:5 w/w of methyl oleate, H_2O_2, and CH_2O_2, respectively. It was done at room temperature under reflux for 16 h along with the controlled addition of H_2O_2 during the first hour of the reaction in

Table I. Recipes for the Emulsion Copolymerization Process of VPi and MAMO

Latex	Water (g)	SLS (g)	MAMO (g)	VPi (g)	$NaHCO_3$ (g)	KPS (g)
PVPi	45.0	0.22	0.00	20.00	0.050	0.05
PVPiMAMO2.5%	45.0	0.54	0.51	19.50	0.124	0.126
PVPiMAMO5%	45.0	0.86	1.10	19.00	0.198	0.202
PVPiMAMO10%	45.0	1.50	2.15	18.00	0.346	0.354
PVPiMAMO25%	45.0	3.42	5.15	15.00	0.790	0.810

an ice bath and with vigorous stirring of the reaction medium (1200 rpm).

MAMO was formed from the reaction between the epoxidized methyl oleate and MA in a ratio of 2:1 w/w, respectively. The reaction was carried out under a constant stirring agitation of 1000 rpm and reflux for 6 h at 100 °C with 0.6% $C_6H_4(OH)_2$ in relation to the total system mass to prevent the polymerization of MA.

Emulsion Polymerization Process

Polymerization reactions were carried out in a three-necked, 250 mL, round-bottom flask under constant magnetic stirring; the flask was connected to a reflux condenser linked to a cold-water stream, a sampling device, and a IKA C-MAG HS 7 hotplate (IKA Works, Inc.) equipped with an integrated temperature control and a Pt1000 temperature probe, which was used to maintain a medium constant temperature. Initially, the emulsifier (sodium dodecyl sulfate), initiator of polymerization (KPS), and buffer ($NaHCO_3$) were added to the reaction system under a constant magnetic stirring of 300 rpm. When the reaction temperature reached a pre-established value of 80 °C, the VPi monomer and MAMO were fed into the reaction flask. The amount of reagents used is listed in Table I. At regular reaction times, a small portion of the reaction, approximately 1 g of the reaction medium, was withdrawn from the reaction system, and about 300 ppm of $C_6H_4(OH)_2$ was added to the samples to prevent polymerization. We determined the reaction conversion on the basis of the gravimetric measurement by drying the reaction samples until a constant weight was maintained in an oven kept at 60 °C. When necessary, gravimetric conversions were corrected by NMR calculation.

Characterization Techniques

The reaction conversion was determined from gravimetric measurements. Dried polymer samples were characterized with differential scanning calorimetry (DSC) and thermogravimetric analysis (thermogravimetry/differential thermal analysis), gel permeation chromatography (GPC), and NMR, and the polymer latex was analyzed by dynamic light-scattering technique.

The thermal stability of the polymeric materials was evaluated on a Shimadzu thermogravimetric analyzer (DTG-60, Shimadzu Scientific Instruments, Columbia, MD) in the temperature range 30–800 °C at a heating rate of 10 °C/min under a nitrogen atmosphere with a flow rate of 30 mL/min. T_g was determined through DSC analyses to obtain T_g performed on a Shimadzu DSC-60 (Shimadzu Scientific Instruments) under a nitrogen atmosphere with a temperature range of −50 to 200 °C at a heating rate of 10 °C/min.

Dynamic light-scattering analyses were performed on a ζ-potential analyzer (model 90Plus, Brookhaven Instruments Corp., Holtsville, NY) to determine the average diameter and particle size distribution of the polymer lattices.

GPC was used for the determination of the MMDs, average molar masses [mass-average molar mass (M_w) and number-average molar mass (M_n)], and molar mass dispersity ($Đ$) values. GPC analyses were performed on a high-performance liquid chromatograph (Shimadzu Scientific Instruments) equipped with a refractometer detector (RID-10A), an inline degasser, a pump (LC-20AD), an autosampler and oven (CTO-20A) with an injection loop of 100 µL, and three separation columns (GPC-803, GPC-804, and GPC-805) with tetrahydrofuran as the mobile phase at 40 °C at a flow rate of 1 mL/min. The calibration curve was built according to polystyrene standards with an average molar mass in the range of 2.5×10^3 to 1.35×10^6 g/mol and a $Đ$ value close to 1.0. Dried polymer samples were solubilized in tetrahydrofuran (0.65 g/L) and filtered through 0.45-µm porous membrane filters before analysis.

The NMR spectra used for elucidating the structure of MAMO and the composition of the polymeric materials were obtained on a Varian Mercury Plus M 300-MHz equipment (Varian Instruments) equipped with a 54-mm probe operating at 300 MHz. Approximately 20-mg samples were dissolved in 1 mL of deuterated chloroform ($CDCl_3$), and the spectra was acquired at 25 °C with tetramethylsilane (TMS) as the internal standard.

RESULTS AND DISCUSSION

The effect of the MAMO concentration on the VPi/MAMO copolymerization is depicted in Figure 1. We observed that elevated conversions close to 100% were achieved when MAMO was added to the reaction mixture in the range from 2.5 to 25 wt %. According to the experimental data shown in Figure 1, high reaction rates were observed; this led to the formation of an increased quantity of polymer latex in a shorter time period. Although high conversions were obtained, the amount of initiator in the reaction medium needed to be increased as a response to the addition of MAMO. On the basis of the experimental results, the higher the concentration of MAMO was, the higher must the concentration of KPS in the reaction medium needed to be; this was probably a result of the presence of chemical impurities obtained from the MAMO synthesis. In turn, this contributed to a decrease in the copolymerization yield.[15,16] We also observed that (co)polymeric lattices with

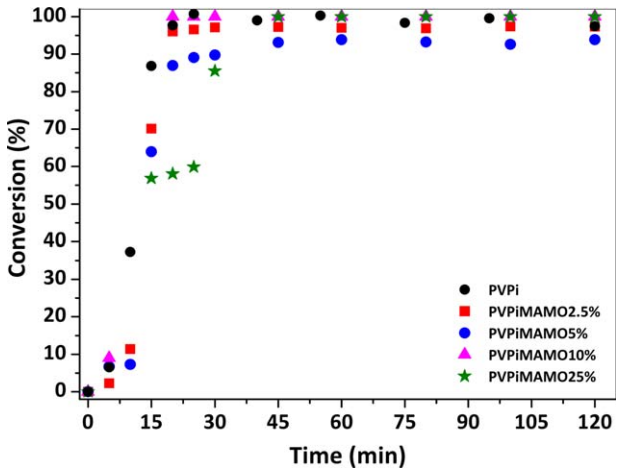

Figure 1. Conversion profiles of the copolymerization reactions with different concentrations of VPi and MAMO. [Color figure can be viewed in the online issue, which is available at wileyonlinelibrary.com.]

high colloidal stability were successfully formed. The (co)polymer lattices, with an average particle diameter ranging from 63 to 101 nm, presented low polydispersity index values; this indicated the formation of (co)polymer nanoparticles with a narrow particle size distribution, as shown in Table II. The observed diminution in the average particle size of the copolymer particles was closely linked to the concentration of emulsifier in the reaction medium responsible for the formation of a greater number of micelles, as the amount of SLS increased.

MAMO synthesis requires high concentrations of $C_6H_4(OH)_2$ to prevent acrylic acid polymerization. After the purification of MAMO with NaOH solution, we expected that a very small amount of $C_6H_4(OH)_2$ would remain dispersed in the monomer. Because it is a polymerization inhibitor, a very small concentration of $C_6H_4(OH)_2$ played a significant role in the reaction behavior during the early stages of the copolymerization; this led to the reduction of the reaction rate as a result of its combination with the radicals of initiators. In this case, when the concentration of MAMO was augmented, high conversions were achieved only when the initiator concentration was also increased. Because of the compartmentalized nature of emulsion polymerization systems, we greatly expected that $C_6H_4(OH)_2$ would promptly act like a scavenger agent on the free radical formed at the very early stages of the polymerization and retard the beginning of the reaction.

The reduction in the polymerization rate could be explained by the decrease in the nucleation process of the particles. As described by Jensen *et al.*,[16] the low solubility in the aqueous continuous medium of OA-based monomers, such as MAMO, may affect the mass-transfer mechanism responsible for the diffusion of MAMO from the monomer droplets through the aqueous phase to the growing polymer particles. It was important to keep in mind that the existence of residual OA also contributed to the decrease in the polymer particle growth rate; this was due to the high probability of a reaction between a free radical and the double bond of the OA aliphatic chain. This led to the formation of very stable radicals presenting a lower propagation constant, which would delay the polymerization.

The MAMO synthesized in accordance with the synthetic route described by Jensen *et al.*[16] was analyzed by NMR measurements, as illustrated in Figure 2. The spectrum of MAMO presented the following chemical shifts:

MAMO: ^{1}H-NMR ($CDCl_3$, δ): 0.88 (3H, H_{11}), 1.10–1.30 [26H, (CH_2)], 1.51–1.61 (4H, $H_{5,6}$), 1.99 (3H, H_{10}), 2.31 (2H, H_2), 3.60 (3H, H_1), 4.00 (1H, H_3), 5.00 (1H, H_4), 5.6 (1H, H_8), 6.15 (1H, H_9).

VPi: ^{1}H-NMR ($CDCl_3$, δ): 1.20 (9H, H_4), 4.56 and 4.57 (1H, H_2), 4.88 and 4.90 (1H, H_3), 7.28 (1H, H_1).

Figure 3 shows the ^{1}H-NMR spectra of the polymeric materials. It was evident that, when compared to the spectrum obtained for the VPi homopolymer, the disappearance of the peaks in these spectra were related to the instaurations present in both the VPi and MAMO monomers (δ = 5.6 and 6.1 ppm; Figure 2), and the appearance of peaks (δ = 3.6, 2.1 and 2.4 ppm) was related to MAMO [Figure 3(C–F)] [Figure 3(B)]. Several spectral changes were observed in the spectra obtained for the different polymers. As the fraction of MAMO in the copolymer chains increased, we observed a reduction in the amount hydrogen of used to quantify the VPi present in the polymeric chains (δ = 4.6–5.0 ppm). On the other hand, the hydrogens characteristic of MAMO increased; this reflected the incorporation of MAMO into the copolymer chains (δ = 3.6 ppm). Equation (1) was used for copolymer characterization[31]:

Table II. Compositions, T_g Values, Average Particle Sizes, Average Molar Masses, and $Đ$ Values of the VPi-Containing Polymeric Materials

Sample	MAMO fraction in feed (mol %)	MAMO fraction in the copolymer (mol %)	T_g (°C)	Average particle size (nm)	Polydispersity index	M_w (g/mol)	M_n (g/mol)	$Đ$
PVPi	0.0	0.0	80.5	101.0 ± 0.4	0.052	1,655,418	763,488	2.17
PVPiMAMO2.5%	0.8	0.2	71.4	109.6 ± 0.4	0.061	1,664,234	1,029,275	1.62
PVPiMAMO5%	1.8	0.6	66.2	117.9 ± 0.4	0.052	895,958	521,426	1.72
PVPiMAMO10%	3.7	2.6	53.8	86.6 ± 0.3	0.114	755,268	475,426	1.59
PVPiMAMO25%	9.9	9.0	38.7	62.6 ± 0.1	0.094	289,628	186,341	1.55

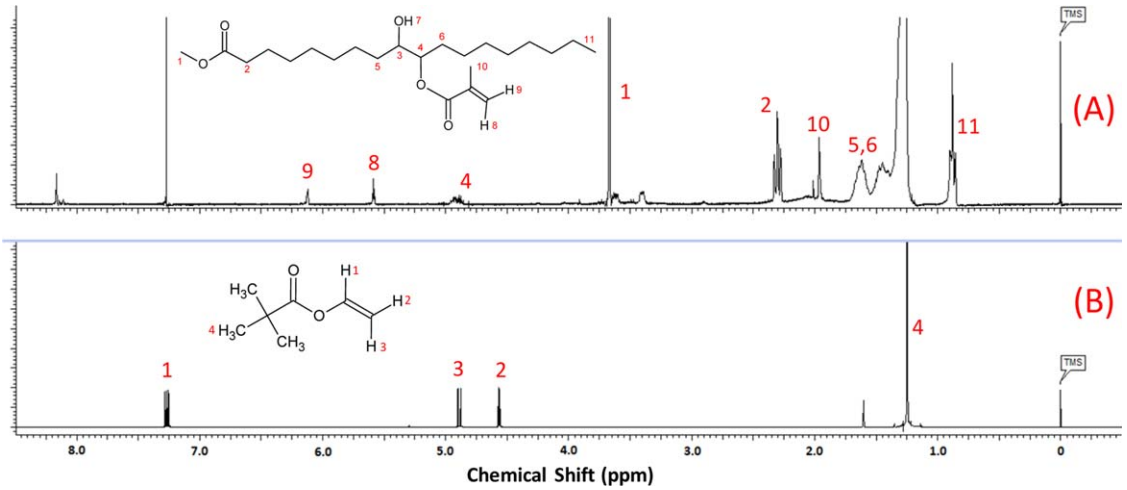

Figure 2. ^{1}H-NMR spectra of the MAMO and VPi monomers. [Color figure can be viewed in the online issue, which is available at wileyonlinelibrary.com.]

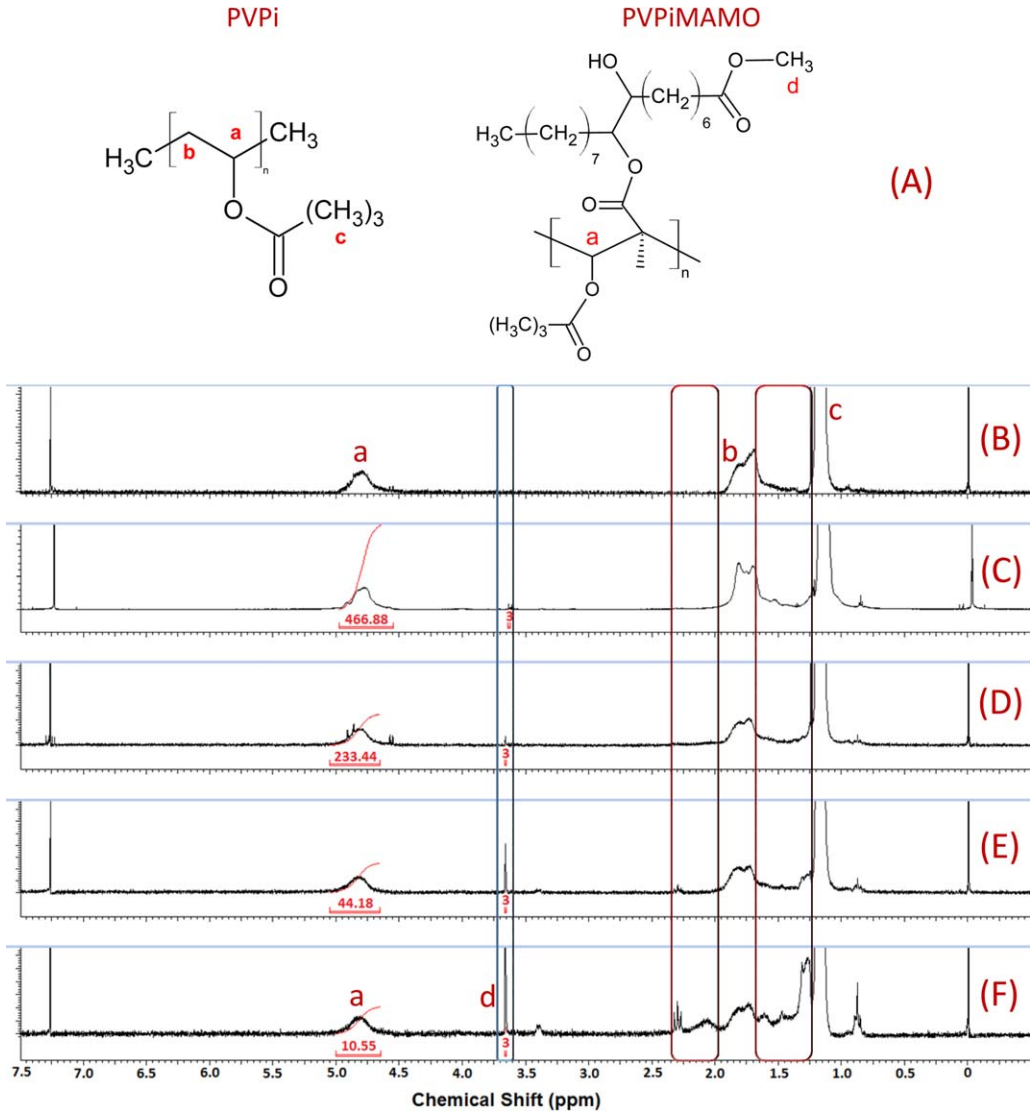

Figure 3. (A) Structural representations of the VPi homopolymer and the VPi/MAMO copolymer. (B–F) ^{1}H-NMR spectra of the polymeric materials: (B) PVPi homopolymer sample, (C) PVPiMAMO2.5% copolymer sample, (D) PVPiMAMO5% copolymer sample, (E) PVPiMAMO10% copolymer sample, and (F) PVPiMAMO25% copolymer sample. [Color figure can be viewed in the online issue, which is available at wileyonlinelibrary.com.]

$$\chi_{MAMO} = \frac{N_a I_{H_d}}{N_a I_{H_d} + N_d I_{H_a}} \quad (1)$$

where χ_{MAMO} is the molar fraction of MAMO in the copolymers, I_{HD} is the integral value for the peak marked with the letter d (MAMO) in the molecular structure in Figure 3, I_{HA} is the integral value for the peak marked with the letter a (VPi) in the molecular structure in Figure 3, N_a is the number of protons related to peak a, and N_d is the number of protons related to peak d.

The final copolymer composition determined according to the procedure proposed by Eren and Küsefoğlu[31] is illustrated in Table II. The experimental data showed that MAMO was significantly incorporated into the copolymer chains, which exhibited a composition of approximately 9 mol % (23.5 wt %) when the initial fraction of MAMO in the reaction medium was equal to 25 wt %. These results were very significant, as copolymerization with high amounts of MAMO could be performed with high polymer yields.

Additional VPi/MAMO batch copolymerizations were carried out to provide the MAMO composition profiles along the reaction time, as follows (see Figures 4 and 5). For copolymer sample PVPiMAMO5%B, the reaction mixture contained 45.0 g of water, 0.86 g of SLS, 1.02 g of MAMO, 19.05 g of VPi, 0.101 g of $NaHCO_3$, and 0.084 g of KPS. For copolymer sample PVPiMAMO10%B, the polymerization was performed with 45.0 g of water, 1.50 g of SLS, 2.03 g of MAMO, 18.03 g of VPi, 0.150 g of $NaHCO_3$, and 0.130 g of KPS.

Even after treatment with the NaOH solution, we also observed that the aforementioned scavenger distinctly affected the polymerization behavior, mainly in the beginning of the reaction because of undesirable small fluctuations in the $C_6H_4(OH)_2$ amount in different batches performed for the synthesis of MAMO. Additionally, the amount of impurities present in the precursor OA also varied, depending on the supplier and/or the vegetable oil source. For this reason, the second set of copolymerization reactions required a smaller amount of initiator in comparison with the previous experimental runs. It is important to emphasize that the batch copolymerization carried out with the same operational conditions of Table I was conducted on a thermal runway. Despite this, similar reaction behavior was observed with a high conversion (ranging from 80 to 90%) and very similar T_g values (≈62 and ≈47 °C) and final copolymer compositions (1.8 and 5.0 mol %) for samples PVPi MAMO5%B and PVPiMAMO10%B, respectively.

Figure 4 shows the conversion and composition profiles of the VPi/MAMO copolymerization. We observed that high reaction conversions took place. Composition drifts were also observed because of the differences in the reactivity between the monomer species; this led to the formation of VPi/MAMO copolymers with heterogeneous compositions throughout the batch. This results show that copolymers presenting a constant composition along the reaction could be obtained only if a control strategy was adopted, for example, one based on the determination of optimum monomer feed rate profiles. Figure 5 outlines the quantitative ^{1}H-NMR measurements of copolymer samples

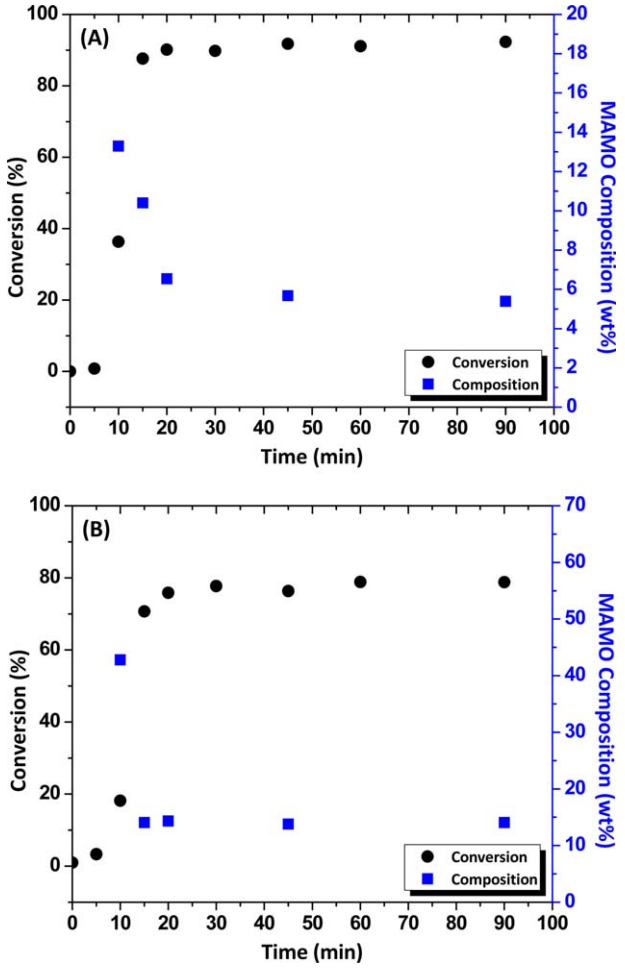

Figure 4. Conversion and composition profiles for the VPi/MAMO copolymerization: (A) For copolymer sample VPiMAMO5%A and (B) For copolymer sample VPiMAMO10%B. [Color figure can be viewed in the online issue, which is available at wileyonlinelibrary.com.]

throughout the polymerization reaction. The copolymer composition was determined on the basis of eq. (2)[32]:

$$\frac{I_{MAMO}}{N_{MAMO}} \times \frac{M_{MAMO}}{m_{MAMO}} = \frac{I_{std}}{N_{std}} \times \frac{M_{std}}{m_{std}} \quad (2)$$

where I_{MAMO} and I_{std} correspond to the integral values of the MAMO and standard (benzoic acid), respectively; N_{MAMO} and N_{std} are related to the number of protons at a chemical shift in the MAMO and standard, respectively; M_{MAMO} and M_{std} are the molar masses of the MAMO and standard, respectively; and m_{MAMO} and m_{std} are the masses of the MAMO and standard (g), respectively.

According to the dynamic composition profiles presented in Figure 4, MAMO was preferentially incorporated into the VPi/MAMO copolymer chains. The composition drifts along the reaction course indicated that the VPi/MAMO copolymer chains were richer in the most reactive monomer (MAMO) in the beginning of the reaction and became richer in the least reactive species (VPi) at the end of the polymerization reaction. The final copolymer compositions of 5.39 wt % (1.80 mol %) for sample PVPiMAMO5%B and 14.06 wt % (5.00 mol %) for

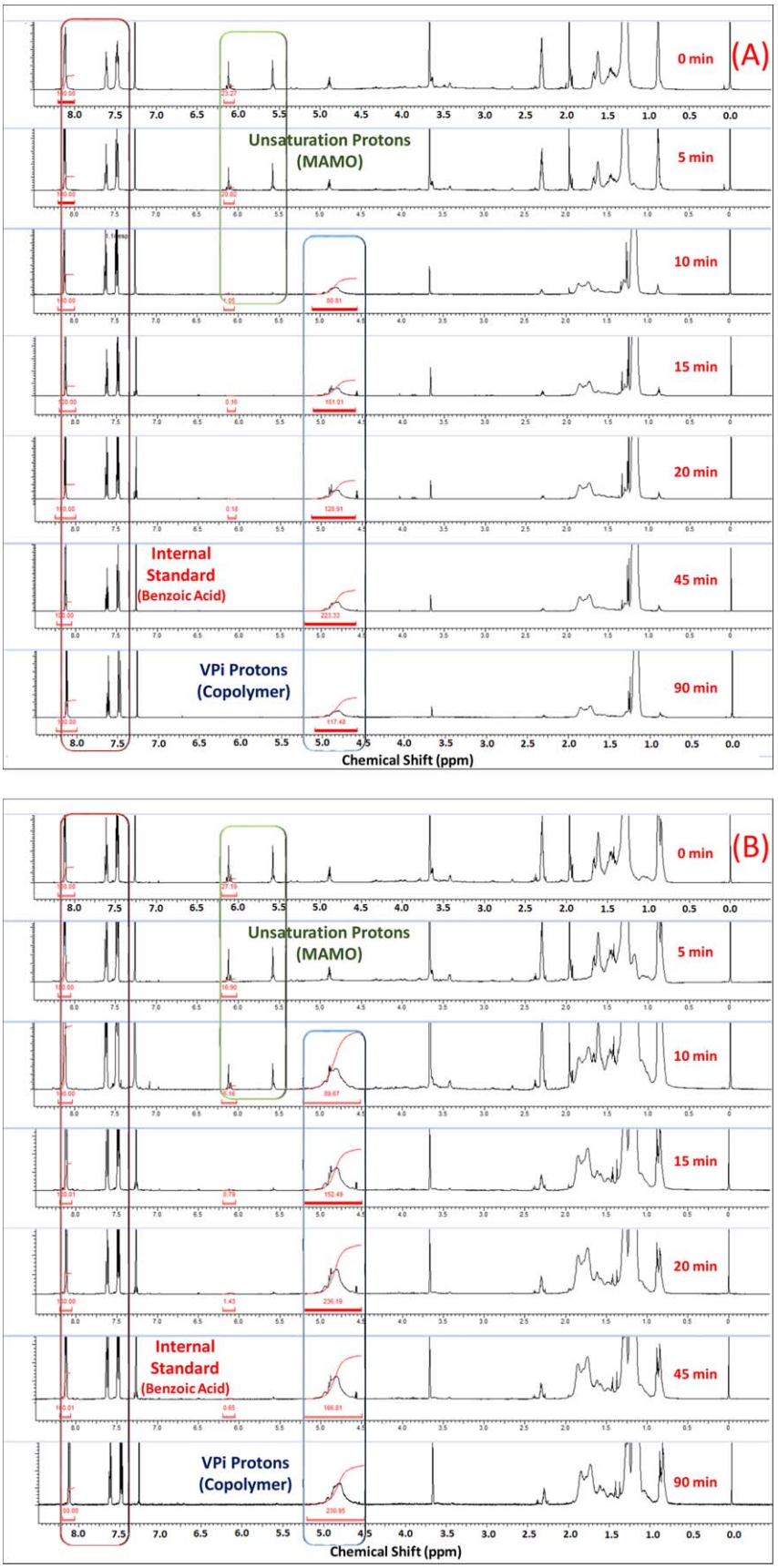

Figure 5. Quantitative ^{1}H-NMR measurements of copolymer samples throughout the polymerization reaction: (A) PVPiMAMO5%B and (B) PVPiMAMO10%B. [Color figure can be viewed in the online issue, which is available at wileyonlinelibrary.com.]

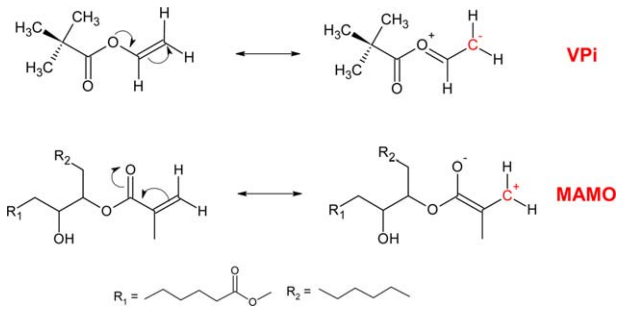

Figure 6. Resonance structures for the VPi and MAMO monomers. [Color figure can be viewed in the online issue, which is available at wileyonlinelibrary.com.]

sample PVPiMAMO10%B were very consistent with the experimental results presented in Table I. The very small differences were attributed to the range of maximum experimental conversion, which was approximately 90% for PVPiMAMO5%B and 80% for PVPiMAMO10%B; these values were lower than the final conversion shown in Figure 1.

With the chemical structure of both VPi and MAMO, it was reasonable to believe that a stereo effect, for instance, of the long carbon chains present in the MAMO structure and strong steric effects of the tertiary butyl group[33,34] from VPi, played a fundamental role in the monomer reactivities. The high reactivity of MAMO in relation to VPi could be interpreted in accordance with the point of view of Dossi *et al.*,[35] where the propagation kinetics during VAc/MMA free-radical copolymerization were investigated by the combination of an experimental study with computational modeling on the basis of quantum chemistry (with density functional theory calculations to evaluate the exchange and correlation energy). According to Dossi *et al.*,[35] one can explain the higher reactivity of MMA in comparison to VAc by taking into consideration the resonance structures of the monomer molecules. According to the resonance structures of VPi and MAMO presented in Figure 6, we noticed a similarity in the reactive groups (VPi and VAc vs MAMO and MMA). Because the reactive carbon atom of the molecular structure of MAMO exhibited a more positive character than the one present in the VPi structure, the MAMO monomer tended to react more easily with radicals present in the reaction medium. In other words, it was more likely that a radical attacked the MAMO double bound when compared to the action of a radical on the VPi double bond; this indicated that MAMO was the most reactive monomer.

Figure 7 shows the effect of the MAMO concentration on the MMDs of the VPi/MAMO copolymers; it clearly indicates that both the MMD and average molar masses were significantly affected by MAMO. The VPi/MAMO copolymers exhibited low values of molar masses as the molar fraction of MAMO in the copolymer chains increased. It is important to emphasize that VPi/MAMO copolymerization was carried out in the absence of chain-transfer agents so we could observe only the major effect of MAMO on the MMD and average molar masses of the copolymers. These results were corroborated by the average molar masses obtained elsewhere in the emulsion copolymerization of vinyl monomers with modified vegetable oils.[15,16]

$Đ$ of the copolymer also decreased as the MAMO molar fraction increased as a result of termination by a combination mechanism.[36,37] $Đ$ of the copolymer decreased from 2.2 to 1.6, and its value was very near the theoretical value of 1.5, where termination took place exclusively via combination. In this particular case, it is important to keep in mind that very small copolymer chains can undergo termination reactions after a combination kinetic mechanism. For this reason, it was reasonable to assume that a mixed kinetic mechanism, which was characterized by terminations by both disproportionation ($Đ = 2.0$) and combination ($Đ = 1.5$), was present.[38,39]

The KPS concentration also played an important role in the average molar masses of the VPi/MAMO copolymers. We expected that an increase in the KPS amount in the reaction medium would lead to an increase in the radical entry rate into the polymer particles and, consequently, to a high termination rate, which would result in copolymer chains presenting low molar masses. As matter of fact, as the initiator concentration was increased, the number of free radicals of initiator in the aqueous phase also increased; this significantly contributed to the increase in the rate of radical entry into the particles and, consequently, to a decrease in the average molar masses of the copolymers.

To determine the effect of MAMO on the macromolecular properties of the copolymer, GPC analyses were performed with a low-molar-mass separation column. In these particular GPC measurements, the separation of low-molar-mass chains was the main interest. Figure 8(A,B) is useful for explaining why the T_g and average molar mass values decreased as the MAMO concentration in the reaction medium increased; this reflected the significant increase in the mass fraction of polymeric chains of a low molar mass. For example, a copolymer containing a molar fraction equal to 9% (or 23.5 wt % in polymer sample PVPiMAMO25% in Table II) consisted of about 35 wt % low-molar-mass chains [Figure 8(B)].

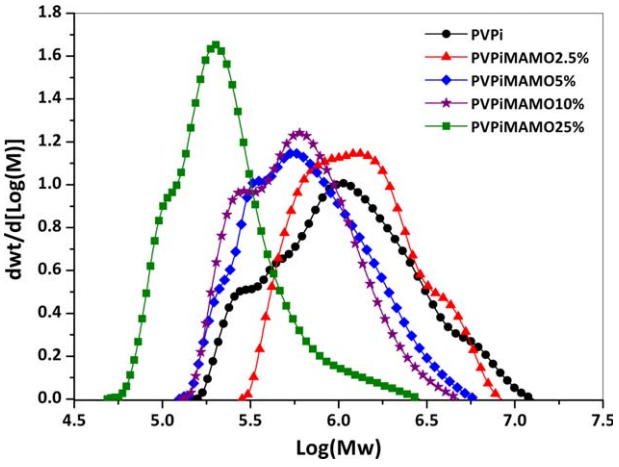

Figure 7. MMDs of the VPi-containing polymeric materials. [Color figure can be viewed in the online issue, which is available at wileyonlinelibrary.com.]

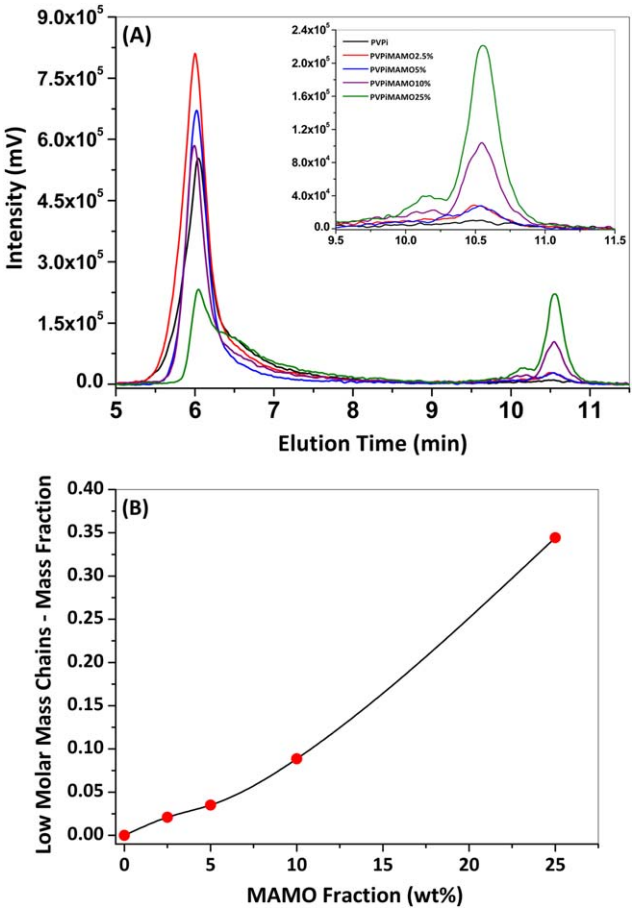

Figure 8. GPC characterization: separation profiles and effects of MAMO on the formation of copolymeric chains with a low molar mass. [Color figure can be viewed in the online issue, which is available at wileyonlinelibrary.com.]

In summary, the average molar masses of copolymers may have been affected by a series of factors, including

1. The initiator concentration, which affected the number of free radicals of initiator in the aqueous phase and significantly contributed to the increase in the rate of radical entry into the polymer particles. This was accompanied by a high termination rate, which reduced the molar masses of the copolymers.
2. The plasticizing effect of MAMO, which increased the molecular mobility and reduced the gel effect. This consequently led to a decrease in the average molar masses of the copolymers when the MAMO concentration in the reaction medium was increased.
3. The reaction of the free radical with the nonepoxidized double bond of the OA aliphatic chain.
4. Chain transfer to oleic and/or impurities, which led to a reduction in the molar mass.

Figure 9 shows the T_g values of the MAMO (Sample PMAMO) and VPi homopolymers along with those of the polymeric materials containing MAMO. According to the measurements obtained via DSC, the observed T_g value for the MAMO homopolymer was equivalent to −20.5 °C (the polymerization was performed with 12.0 g of water, 1.0 g of SLS, 3.3 g of MAMO, 19.05 g of VPi, 0.06 g of $NaHCO_3$, and 1.0 g of KPS at 80 °C for 8 h). The T_g of the MAMO homopolymer was very low in comparison to the T_g determined for the VPi homopolymer (80.5 °C).

With respect to the VPi/MAMO copolymers, we firmly expected that T_g was significantly affected by the chemical structure of the polymer chains. The MAMO composition had a dominant and more influential impact on the T_g of the VPi/MAMO copolymers. As the MAMO fraction increased in the copolymer chains, the T_g of the copolymer decreased. The higher the MAMO concentration was, the lower the T_g of copolymers was; hence, they were inversely proportional. Therefore, the mobility of the copolymer chains was enhanced by MAMO compared to that of the VPi homopolymer chains. The incorporation of MAMO into the polymer chains resulted in a significant decrease in the T_g of the final material; this was approximately a 40 °C reduction [for sample PVPiMAMO25%, the molar fraction of MAMO in the copolymer chains was approximately 9% (or 23.5 wt %) with a T_g equal to 39 °C (see Table II)] in comparison to the T_g value observed for the pure PVPi.

As shown in Table II, it seemed that the observed reduction in the T_g values was related to the molar mass of the copolymers. However, with the range of average molar masses, only a very

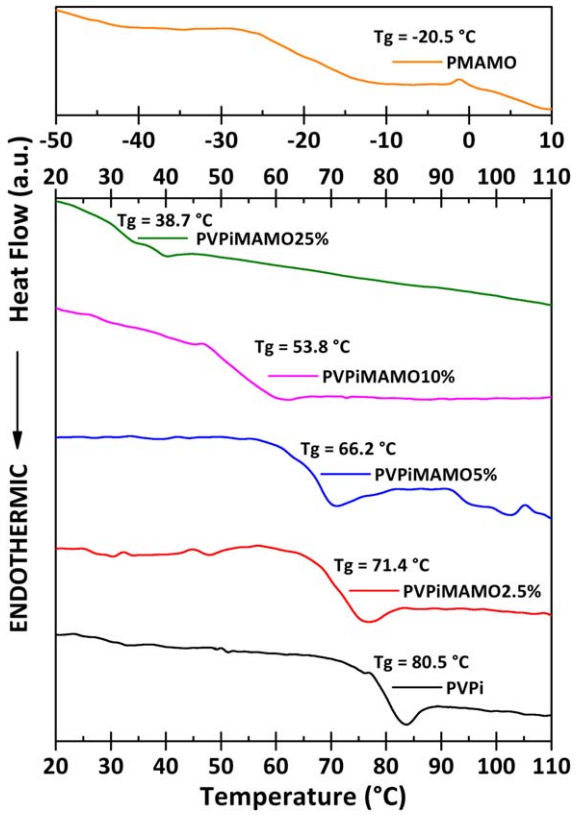

Figure 9. T_g values of the VPi-containing polymeric materials. [Color figure can be viewed in the online issue, which is available at wileyonlinelibrary.com.]

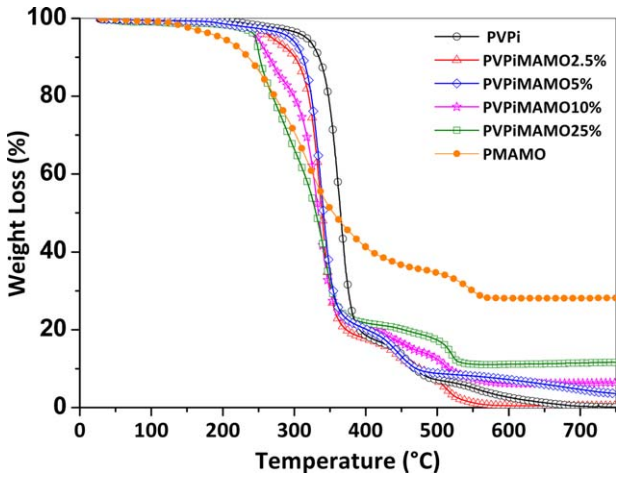

Figure 10. Thermogravimetric analysis of the VPi-containing polymeric materials. [Color figure can be viewed in the online issue, which is available at wileyonlinelibrary.com.]

limited effect of the VPi/MAMO copolymeric chains containing a low molar mass on the T_g was expected. In other words, the reduction in the average mass molar of the copolymeric materials [from $\approx 1.66 \times 10^6$ g/mol for the VPi homopolymer (sample PVPi) to $\approx 2.90 \times 10^5$ g/mol for the VPi/MAMO copolymer containing 9 mol % MAMO (sample PVPiMAMO25%)] was insufficient for explaining the vast differences observed here, which were closely associated with the MAMO fractions. These experimental results show that the T_g values of the copolymers could be easily tailored and controlled by the insertion of MAMO molecules into the polymer chains; this showed favorable concordance with the experimental data obtained by Jensen *et al.*[16] for styrene/acrylated methyl oleate copolymers and Ferreira *et al.*[15] for soybean-oil-based polymers copolymers [containing a mixture of acrylated linolenic acid, linoleic acid, and OA Acrylated free fatty acids mixture (AFFAM) in combination with MMA] from the emulsion polymerization process.

Figure 10 presents the thermal stability and weight loss profiles of MAMO-based polymeric materials determined through thermogravimetric measurements. The polymeric materials exhibited good thermal stability, undergoing full degradation in the interval from 230 to 650 °C with two important weight losses, depending on the MAMO molar fraction. The first significant weight loss was observed between 250 and 400 °C, and the second significant weight loss was observed between 400 and 650 °C. Additionally, we also observed that the thermal stability of the copolymers decreased slightly when the MAMO concentration was increased in the reaction medium. The copolymers (PVPiMAMO10% and PVPiMAMO25%) were not completely degraded; this indicated the formation of a crosslinked material when the incorporation of MAMO into the polymeric chains was increased.[15] Both DSC measurements and thermogravimetric analyses seemed to indicate that the VPi/MAMO copolymers may have presented a nonhomogeneous structure; this indicated that the final copolymer chains might have exhibited a complex macromolecular arrangement. Despite this, we expected the formation of copolymer chains to present a random structure.

CONCLUSIONS

In this study VPi/MAMO copolymers were successfully synthesized through a batch emulsion polymerization process. According to the experimental results, high final conversions and an elevated incorporation of MAMO into the final copolymer chains were achieved, independently of the MAMO concentration in the reaction medium. We observed that the incorporation of MAMO into the copolymer chains significantly decreased T_g; this suggested that MAMO has high potential for use in coatings and adhesives. GPC characterization showed that the fraction of polymer chains of low molar mass increased when the concentration of MAMO increased. This led to a decrease in the average molar masses, the narrowing of MMD, and the diminution of $Đ$.

ACKNOWLEDGMENTS

The authors thank Coordenação de Aperfeiçoamento de Pessoal de Nível Superior and Conselho Nacional de Pesquisa e Desenvolvimento for financial support and scholarships. In particular, one of the authors (F.M.) thanks Empresa Brasileira de Pesquisas Agropecuárias, Laboratório de Materiais e Combustíveis, and Laboratório de Química Medicinal e Tecnológica for research support.

REFERENCES

1. Chirowodza, H.; Zou, M.; Sanderson, R. D. *J. Appl. Polym. Sci.* **2010**, *117*, 3460.
2. Lee, S. G.; Kim, J. P.; Lyoo, W. S.; Kwak, J. W.; Noh, S. K.; Park, C. S.; Kim, J. H. *J. Appl. Polym. Sci.* **2005**, *95*, 1539.
3. Lyoo, W.; Park, C.; Yeum, J.; Ji, B.; Lee, C.; Lee, S.; Lee, J. *Colloid Polym. Sci.* **2002**, *280*, 1075.
4. Lyoo, W. S.; Cha, J. W.; Kwak, K. Y.; Lee, Y. J.; Jeon, H. Y.; Chung, Y. S.; Noh, S. K. In 5th International Conference on Times of Polymers (TOP) and Composites; Damore, A., Acierno, D., Grassia, L., Eds.; Ischia, Italy.; **2010**; p 389.
5. Nguyen, T. L. U.; Farrugia, B.; Davis, T. P.; Barner-Kowollik, C.; Stenzel, M. H. *J. Polym. Sci. Part A: Polym. Chem.* **2007**, *45*, 3256.
6. Lyoo, W. S.; Kwak, J. W.; Yeum, J. H.; Ji, B. C.; Lee, C. J.; Noh, S. K. *J. Polym. Sci. Part A: Polym. Chem.* **2005**, *43*, 789.
7. Lyoo, A. S.; Park, C. S.; Choi, K. H.; Kwak, J. W.; Yoon, W. S.; Noh, S. K. *Polym. Plast. Technol. Eng.* **2005**, *44*, 475.
8. Araujo, R. T.; Ferreira, G. R.; Segura, T.; Souza, F. G., Jr.; Machado, F. *Eur. Polym. J.* **2015**, *68*, 441.
9. Lyoo, W. S.; Han, S. S.; Kim, J. H.; Yoon, W. S.; Lee, C. J.; Kwon, I. C.; Lee, J.; Ji, B. C.; Han, M. H. *Angew. Makromol. Chem.* **1999**, *271*, 46.
10. Lyoo, W. S.; Kim, B. C.; Ha, W. S. *Polym. J.* **1998**, *30*, 424.
11. Song, D. H.; Lyoo, W. S. *J. Appl. Polym. Sci.* **2007**, *104*, 410.
12. Kikuchi, K.; Kitawaki, M.; Suzuki, A.; Oku, T. *J. Colloid Interface Sci.* **2009**, *338*, 480.
13. Kwark, Y. J.; Lyoo, W. S.; Ha, W. S. *Polym. J.* **1996**, *28*, 851.

14. Suzuki, S.; Kikuchi, K.; Suzuki, A.; Okaya, T.; Nomura, M. *Colloid Polym. Sci.* **2007**, *285*, 523.
15. Ferreira, G. R.; Braquehais, J. R.; da Silva, W. N.; Machado, F. *Ind. Crops Prod.* **2015**, *65*, 14.
16. Jensen, A. T.; Sayer, C.; Araújo, P. H. H.; Machado, F. *Eur. J. Lipid. Sci. Technol.* **2014**, *116*, 37.
17. Lligadas, G.; Ronda, J. C.; Galià, M.; Cádiz, V. *J. Polym. Sci. Part A: Polym. Chem.* **2013**, *51*, 2111.
18. Meier, M. A. R.; Metzger, J. O.; Schubert, U. S. *Chem. Soc. Rev.* **2007**, *36*, 1788.
19. Montero de Espinosa, L.; Meier, M. A. R. *Eur. Polym. J.* **2011**, *47*, 837.
20. Medeiros, A. M. M. S.; Machado, F.; Rubim, J. C. *Eur. Polym. J.* **2015**, *71*, 152.
21. Gooch, J. W. Emulsification and Polymerization of Alkyd Resins; Springer: New York, **2002**.
22. Wool, R.; Sun, X. S. Bio-Based Polymers and Composites; Academic: London, **2005**.
23. Maassen, W.; Meier, M. A. R.; Willenbacher, N. *Int. J. Adhes. Adhes.* **2016**, *64*, 65.
24. Galià, M.; de Espinosa, L. M.; Ronda, J. C.; Lligadas, G.; Cádiz, V. *Eur. J. Lipid Sci. Technol.* **2010**, *112*, 87.
25. Ronda, J. C.; Lligadas, G.; Galià, M.; Cádiz, V. *React. Funct. Polym.* **2013**, *73*, 381.
26. Moreno, M.; Goikoetxea, M.; Barandiaran, M. J. *J. Polym. Sci. Part A: Polym. Chem.* **2012**, *50*, 4628.
27. Li, F.; Hanson, M. V.; Larock, R. C. *Polymer* **2001**, *42*, 1567.
28. Lovell, A. P.; El-Aaser, M. S. Emulsion Polymerization and Emulsion Polymers; Wiley: Chichester, England, **1997**.
29. Bunker, S. P.; Wool, R. P. *J. Polym. Sci. Part A: Polym. Chem.* **2002**, *40*, 451.
30. de Espinosa, L. M.; Ronda, J. C.; Galià, M.; Cádiz, V. *J. Polym. Sci. Part A: Polym. Chem.* **2009**, *47*, 1159.
31. Eren, T.; Küsefoğlu, S. H. *J. Appl. Polym. Sci.* **2004**, *94*, 2475.
32. Gratia, A.; Merlet, D.; Ducruet, V.; Lyathaud, C. *Anal. Chim. Acta* **2015**, *853*, 477.
33. Nguyen, V. H.; Haldorai, Y.; Pham, Q. L.; Noh, S. K.; Lyoo, W. S.; Shim, J.-J. *Eur. Polym. J.* **2010**, *46*, 2190.
34. Lyoo, W. S.; Kim, J. H.; Choi, J. H.; Kim, B. C.; Blackwell, J. *Macromolecules* **2001**, *34*, 3982.
35. Dossi, M.; Liang, K.; Hutchinson, R. A.; Moscatelli, D. J. *Phys. Chem. B* **2010**, *114*, 4213.
36. Plessis, C.; Arzamendi, G.; Leiza, J. R.; Schoonbrood, H. A. S.; Charmot, D.; Asua, J. M. *Am. Chem. Soc.* **2000**, *33*, 5041.
37. Sayer, C.; Lima, E. L.; Pinto, J. C.; Arzamendi, G.; Asua, J. M. *J. Polym. Sci. Part A: Polym. Chem.* **2000**, *38*, 1100.
38. Schork, F. J. In Polymer Reactor Engineering; McGreavy, C, Ed.; Springer Science: New Delhi, **1994**.
39. Odian, G. Principles of Polymerization; Wiley: Hoboken, NJ, **2004**; p 198.